Experimental Characterization of Wearable Antennas and Circuits for RF Energy Harvesting in WBANs

Henrique M. Saraiva[1], Luís M. Borges[1], Norberto Barroca[1], Jorge Tavares[1], Paulo T. Gouveia[1], Fernando J. Velez[1], Caroline Loss[2] and Rita Salvado[2]
[1] Instituto de Telecomunicações/DEM
[2] Textile and Paper Materials Research Unit
Universidade da Beira Interior
Covilhã, Portugal
{m5212, lborges, d708, m1612, m4788, fjv, d1338, rita.salvado}@ubi.pt

Pedro Pinho[3,4], Ricardo Gonçalves[3,5] and Nuno Borges Carvalho[3,5]
[3] Instituto de Telecomunicações, Aveiro, Portugal
[4] Instituto Superior de Engenharia de Lisboa, Lisboa, Portugal
[5] Universidade de Aveiro, Aveiro, Portugal
ppinho@deetc.isel.pt, rgoncalves@av.it.pt, nbcarvalho@ua.pt

Raúl Chavéz-Santiago and Ilangko Balasingham
Intervention Centre,
Oslo University Hospital
Institute of Clinical Medicine
University of Oslo
Norwegian University of Science and Technology (NTNU)
raul.chavez-santiago@rr-research.no, ilangko@medisin.uio.no

Abstract—**Field trials have been performed in Covilhã to identify the spectrum opportunities for radio frequency (RF) energy harvesting through power density measurements from 350 MHz to 3 GHz. Based on the identification of the most promising opportunities, a dual-band printed antenna was conceived, operating at GSM bands (900/1800), with gains of 1.8 and 2.06 dBi, and efficiency varying from 77.6 to 82%, for the highest and lowest operating frequency bands, respectively. In this paper, guidelines for the design of RF energy harvesting circuits and choice of textile materials for a wearable antenna are briefly discussed. Besides, we address the development and experimental characterization of three different prototypes of a five-stage Dickson voltage multiplier (with and without impedance matching circuit) responsible for RF energy harvesting. All the three prototypes (1, 2 and 3) can power supply the sensor node for RF received powers of 2 dBm, -3 dBm and -4 dBm, and conversion efficiencies of 6, 18 and 20%, respectively.**

I. Introduction

Future improvements in radio frequency (RF) energy harvesting technology will facilitate the creation of wireless body area networks (WBANs) with no need of dedicated transmitters, as a reliable source of wireless energy power [1]. This goal can be accomplished by enabling the capture of electromagnetic energy from multiple available ambient RF energy sources, such as mobile base stations, TV and radio transmitters, and mobile phones. Moreover, since WBAN nodes are battery operated, energy recharging is a possibility, avoiding the need of battery replacement. However, the service lifetime of the electronic components could be a major concern if there is no possibility to collect enough energy to generate the voltage needed to drive the sensor node. Medium access control (MAC) and routing protocols also play an important role in the network performance [2]. Thus, to choose the best energy harvesting opportunities is essential to optimize the overall network performance whilst optimizing the energy consumption. In the context of WBANs, electromagnetic RF energy harvesting is accomplished by using wearable antennas that allow for power supplying the sensor nodes [3]. Ubiquitously available RF sources, at different bands, are therefore exploited for RF electromagnetic energy harvesting purposes.

In this work, we have identified the opportunistic radio frequency bands for RF energy harvesting and considered these frequency bands to conceive multi-band antennas for electromagnetic energy harvesting. Besides, we have briefly addressed the guidelines for the development of wearable flexible antennas and designing circuits to harvest RF energy. In [6], we have designed and simulated antennas and circuits for ambient RF energy harvesting in the context of the PROENERGY-WSN project [4]. This work aims to experimentally characterize the developed wearable antennas and circuits for RF energy harvesting system, which consists of a 5-stage Dickson voltage multiplier with an impedance matching circuit, rectifier and energy storage sub-system.

The remainder of the paper is organized as follows. Section II addresses the spectrum opportunities based on the field trials that were held in Covilhã, Portugal. Section III describes an efficient dual-band antenna for collecting RF energy. Guidelines for the choice of textile materials to be used in future wearable antennas are also briefly presented. Section IV presents the simulation results for the dimensioning of a 5-stage Dickson voltage multiplier. Section V presents the simulation and experimental results of the three prototypes (with and without impedance matching circuit) of the 5-stage Dickson voltage multiplier followed by the discussion of the results. Finally, conclusions are drawn in Section VI.

II. Indoor and Outdoor Spectrum Opportunities

To seek the best spectrum opportunities for RF energy harvesting and development of multi-band antennas, we have conducted several field trial measurements in Covilhã, Portugal, in both indoor and outdoor environments [6]. The complete description of the methods along with 36 locations for power density measurements is presented in [2], [5] and [6].

A. Indoor Opportunities

Figure 1 presents the indoor spectrum opportunities in terms of average received power, P_r, for the higher education institution in Covilhã, the set of frequencies, f, with high energy available for harvesting comprises the range from 934 to 960 MHz (GSM900), 1854 to 1892 MHz (GSM1800), 2116 to 2160 MHz (UMTS), 2359 MHz (amateur, SAP/SAB applications, video), and 2404 to 2468 MHz (Wi-Fi).

This work was supported by the Ph.D. FCT grants FRH/BD/66803/2009, SFRH/BD/38356/2007, by PEst-OE/EEI/LA0008/2013, Marie Curie Reintegration Grant PLANOPTI (FP7-PEOPLE-2009-RG), the European Social Fund (ESF), OPPORTUNISTIC-CR, PROENERGY-WSN, INSYSM, CREaTION, HANDCAD, COST IC0905 "TERRA", COST IC0902 and COST IC1004.

978-1-4799-4482-8/14/$31.00 ©2014 IEEE

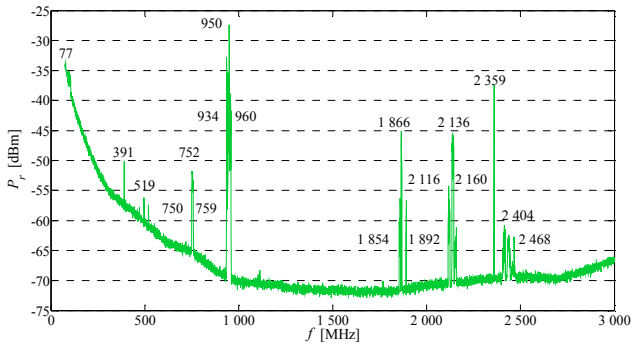

Figure 1. Average received power for the indoor scenario.

B. Outdoor Opportunities

The values of the average received power for the field trials performed in public places are shown in Fig. 2. The set of frequencies with more energy available for harvesting are in the range from 79 to 96 MHz (mobile/radio broadcast stations), 391 MHz (emergency broadcast stations), 750 to 759 MHz (digital television broadcast stations), 935 to 960 MHz (GSM 900 broadcast stations), 1854 to 1870 MHz (GSM 1800 broadcast stations) and 2115 to 2160 MHz (UMTS broadcast stations).

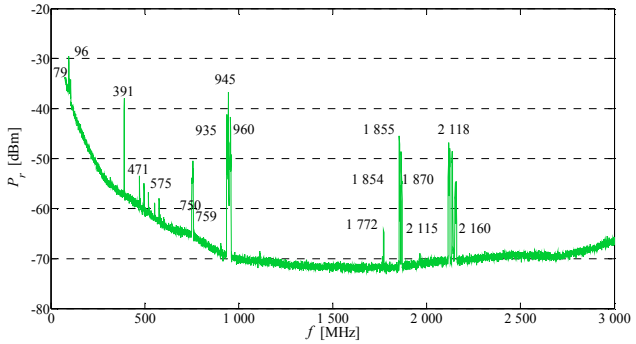

Figure 2. Average received power for the outdoor scenario.

III. Antenna for RF Energy Harvesting

A. Dual-band antenna

In this section, we propose a dual-band antenna suitable for possible implementation within clothes based on spectrum opportunities, as shown in Fig. 3. Table I presents the corresponding antenna dimensions [5]. The *Cordura*® fabric type was considered for the dielectric substrate, presenting a relative permittivity, ε_r, of 1.9, loss tangent, *tan* δ, of 0.0098 and fabric thickness of 0.5 mm at 945 MHz. For the conductive sections of the antenna an electrotextile (*Zelt*), with an electric conductivity 1.75×10^5 S/m was used.

The variation of the simulated and measured return loss is presented in Fig. 4 for the proposed dual-band antenna, considering a return loss S_{11} < -10 dB. The lowest frequency band considered is from 820-1000 MHz, covering the entire E-GSM band, while the highest considered band is in the range 1690-1930 MHz, covering the entire DSC1800 band.

It is a worth noting, however, that the radiation pattern for the dual-band antenna suffers a deformation at 1800 MHz. The obtained radiation pattern in the YZ and XZ planes for the proposed antenna (where dimensions are presented in Fig. 3), is based on numerical simulation and is shown in Fig. 5.

The gains for the dual-band antenna are about 1.8 dBi and 2.06 dBi, with a radiation efficiency of 82% and 77.6% for the lowest and highest operating frequency bands, respectively.

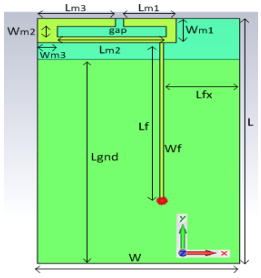

Figure 3. Geometry for the proposed dual-band antenna.

TABLE I. PROPOSED DUAL-BAND ANTENNA DIMENSIONS

Parameter	Dimension [mm]
L, *Lgnd*, *Lf*, *Lfx*	120, 100, 78, 30
Lm1, *Lm2*, *Lm3*, *gap*	21, 43, 31, 3
W, *Wf*, *Wm1*, *Wm2*, *Wm3*	80, 1.5, 12, 5, 8

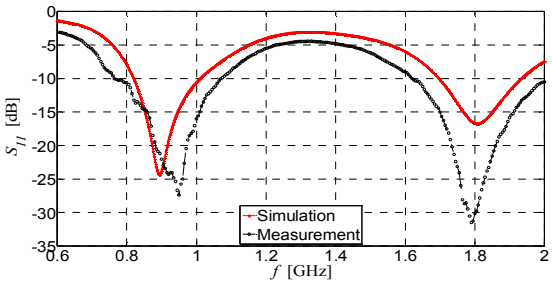

Figure 4. Simulated and measured return loss for the dual-band antenna.

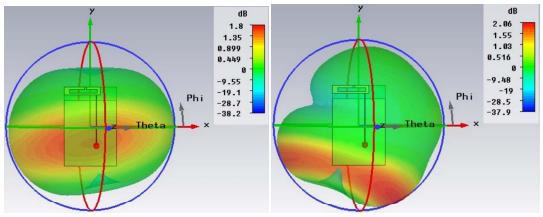

(a) (b)

Figure 5. 3D simulated radiation pattern for the dual-band antenna, including the YZ plane and XZ plane, at a) 900 MHz and b) 1800 MHz.

B. Guidelines to develop wearable flexible antennas

The new generation of garments will be able to perform a continuous monitoring in various fields, such as health [7], communicating the data generated to remote receivers. Wearable antennas are the link that integrates cloths in the communication system, making the integration of electronic devices more discrete and less intrusive.

Specific requirements for wearable antennas (based on textiles) are the planar structure and flexible materials. However, some characteristics of the materials highly influence the performance of the antenna, e.g., the dielectric constant and loss tangent, for a specific frequency, the

thickness, the moisture content in a specific environment (Regain), and the geometrical/mechanical stability of the fabric. In general, ordinary textiles present a low dielectric constant, in between 1 and 2 (as they are very porous).

Guidelines to develop wearable flexible antennas are addressed in [6] and include the following aspects. A low and stable electrical resistance (≤1Ω/square) of the fabric is desired to minimize losses, where the resistance must be homogeneous over the antenna area, i.e., the variance of the resistance must be low. The assembly of the conductive patch with the dielectric substrate is critical [8], and the geometrical dimensions should remain stable when connecting these two components. The fabrics for dielectrics should present a low Regain. For the very narrow parts, the cut should be made in the transverse direction, avoiding the fraying of the yarns [8].

IV. RF Energy Harvesting Circuits

The path loss influences the RF energy harvesting. The Friis free-space equation relates the received power, P_r, at a distance, d, with the transmitted power, P_t, as follows:

$$P_r = P_t \cdot G_t \cdot G_r \cdot (\lambda/4\pi d)^2 \quad (4)$$

where G_t and G_r are the antenna gains of the transmitter and receiver, respectively. Based on equation (4), we can observe that, the received power depends on the frequency (the higher the frequency is the lower the received power is), and decreases with the square of the distance. To conceive an RF energy efficient rectifier which enables to rectify and amplify the input voltage, the Cockcroft-Walton and Dickson voltage multiplier circuits can be considered. This work only addresses the Dickson voltage multiplier, as shown in Fig. 6, since, according to [9], both topologies have a similar performance. In order to have a self-sustainable WBAN, energy efficient harvesting and management techniques must be considered.

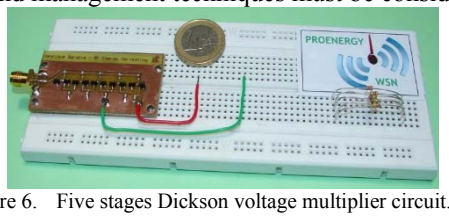

Figure 6. Five stages Dickson voltage multiplier circuit.

However, one of the drawbacks of wireless sensor devices is the finite battery capacity, as well as the voltage generated by the RF energy harvesting circuit, since it may be insufficient to drive the *motes* (at least 1.8V is needed for the IRIS *mote*). By means of simulation, we have addressed the main aspects and parameters that influence the performance of the Dickson voltage multiplier, e.g., the choice of diodes, the number of stages and the load impedance. We have used the Advanced Design System (ADS) [10] from Agilent and varied the RF received power, P_r, from -50 dBm to 20 dBm. The considered centre frequency is equal to 945 MHz since, in this work, we have identified the GSM 900 band as the most promising one for RF energy harvesting. The Dickson voltage multiplier presented in Fig. 6 is mainly formed by diodes and capacitors in parallel. As the input peak voltage from the antenna signal is usually much lower than the diode forward conduction voltage [9], diodes with low turn-on voltage have been considered. Thus, we considered HSMS-2850 Schottky diodes from Avago Technologies optimized for low power applications. The number of rectifier stages has a major impact on the output voltage of the Dickson voltage multiplier. According to [11], the output open circuit voltage (OCV) of an N-stage Dickson voltage multiplier is given by:

$$V_{out} = 2 \cdot N \cdot (V_{in} - V_T) \quad (5)$$

where N is the number of stages, V_{in} is the input voltage amplitude and V_T is the forward conduction voltage of diodes. As shown in equation (5), the output voltage is directly proportional to the number of stages. However, practical restrictions (e.g., conversion efficiency) limit the number of permissible stages. The conversion efficiency, η_0, of a Dickson voltage multiplier is responsible for providing a representation of the overall performance of the circuit, and defines the relationship between the output DC power, P_{DC}, and the RF received power, P_{RF}, as follows:

$$\eta_0[\%] = (P_{DC}/P_{RF}) \cdot 100 \quad (6)$$

where the output DC power is given by:

$$P_{DC} = V_{DC} \cdot I_{DC} \quad (7)$$

V. Simulation and Experimental Results

A. Not Employing Impedance Matching Circuit

Figures 7 and 8 analyse the impact of the number of stages (3, 5 or 8) on the output voltage and conversion efficiency of the Dickson voltage multiplier, by assuming a load impedance of 100 kΩ. These simulation results were obtained through a harmonic balanced analysis (i.e., a frequency domain method) that evaluates the steady state solution of a nonlinear circuit.

By analysing Fig. 7, we conclude that, by increasing the number of stages, we increase the output voltage. The saturation is theoretically obtained by multiplying the number of stages by the reverse breakdown voltage (i.e., 3.8V for HSMS-2850). The maximum output voltage obtained by simulation is approximately 11, 18 and 29 V, respectively, which matches to RF received powers of 10, 12 and 15 dBm.

Figure 8 presents the effect of the RF received power on the conversion efficiency. By adding more stages, the peak of the conversion efficiency curve shifts toward the higher received power region, similarly to the results from [13]. As a consequence, we have chosen the 5-stage Dickson voltage multiplier as the best circuit for RF energy harvesting for WBANs. This is explained by the fact that more than 5 stages will not bring substantial improvement for the power levels considered, due to energy losses along the chain [9]. Moreover, since the wireless sensor nodes need at least 1.8V for operation (i.e., approximately -10 dBm RF input power from simulated results), the 5-stage Dickson voltage multiplier is the one which presents the best performance in terms of conversion efficiency. Consequently, we have decided to conceive a 5-stage Dickson voltage multiplier Prototype 1 in a printed circuit board (PCB) fabricated with two layers by using a FR-4 epoxy glass substrate and evaluate it by using the E8361C PNA Microwave Network Analyser and the Agilent E4433B Signal Generator.

By comparing the simulation (Sim.) and the experimental (Exp.) results, we conclude that there are an average deviation

of 59% between the simulation and experimental results for the output voltage, whereas the experimental saturation value occurs at the RF input received power of 16 dBm.

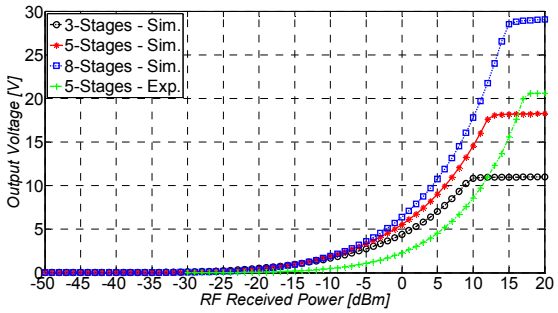

Figure 7. Impact of the number of stages on the output voltage for an *N*-stage Dickson voltage multiplier with a load impedance of 100 kΩ.

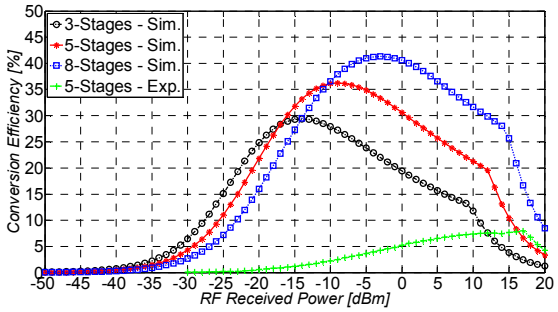

Figure 8. Impact of the number of stages on the conversion efficiency for an *N*-stage Dickson voltage multiplier with a load impedance of 100 kΩ.

Besides, there is an average deviation of 75% between the simulation and experimental results for the conversion efficiency. The maximum conversion efficiency is approximately 8%. We may conclude that the deviations for the output voltage and conversion efficiency can be explained by the impedance mismatching between the antenna and the 5-stage Dickson voltage multiplier prototype, as shown in Fig. 10 from [6]. The prototype measured impedance is Z_{in}=262.49+j401.65 Ω at 945 MHz. In Fig. 10 from [6], it is noticeable that the measured return loss coefficient, S_{11}, is extremely high which induces significant amount of reflection. One solution is to use a single stub matching circuit for improving both the output voltage and conversion efficiency and cancel the losses due to reflection, like in [12], as discussed in next section.

B. Employing Impedance Matching Circuit

In [6], the impact of the load impedance on the conversion efficiency of the 5-stage Dickson voltage multiplier is discussed and analysed. From [6], we are able to conclude that the optimal conversion efficiency is achieved when the load impedance is 50 kΩ. If the resistive load value is too low or too high, the conversion efficiency significantly decreases.

In WBAN the nodes equivalent impedance is different for each radio operation state (RX, TX and SLEEP). According to [12], the value of the impedance from Mica2 mote in the deep sleep state is 100 kΩ. The reference impedance load for the IRIS motes is also 100 kΩ. Hence, the impedance matching circuit is designed for an impedance reference load of 100 kΩ. Prototypes 2 and 3 have been developed after testing Prototype 1. Prototypes 2 and 3 are fabricated in the same special RF substrate (i.e., RO4003 from Rogers). Prototype 2 is composed by a 5-stage Dickson voltage multiplier alone, whereas Prototype 3 includes a match impedance circuit. Prototype 3 has a match impedance circuit that takes into account the measured impedance from Prototype 2, i.e., Z_{in}=130+j10.5 Ω at 945 MHz. Thus, Prototype 3 presents a measured impedance of Z_{in}=34.9+j1.66 Ω at 945 MHz.

The envisaged scenario considers two levels for the output voltage: the minimum voltage to power supply the sensor node (i.e., 1.8 V) and the advised voltage to power supply the sensor node (i.e., 3 V), shown in Fig. 9 by orange lines.

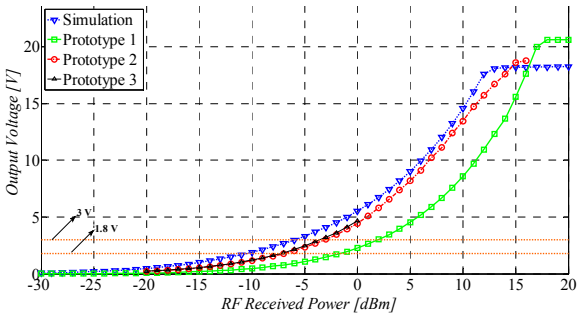

Figure 9. Impact of the RF received power on the output voltage for the 5-stage Dickson voltage multiplier with a load impedance of 100 kΩ.

By observing Fig. 9 we conclude that Prototype 1 presents an average deviation from the simulated values of around 59% in terms of output voltage, whereas the saturation zone occurs at an RF received power of 16 dBm. Both prototypes (2 and 3) present a similar behaviour, but Prototype 3 shows better results compared to Prototype 2 because it benefits from the impedance matching circuit. By comparing the results obtained for Prototypes 2 and 3, the average deviation in terms of output voltage is approximately 24%. In Prototype 3, the saturation zone is not achieved, since previous tests have shown that to increase the RF received power (in the signal generator) to levels higher than 0 dBm may cause burning of the electronic components. This is the reason why we present limited experimental values for Prototype 3. In turn, for Prototype 2 we achieved the saturation zone at 15 dBm, since the match impedance circuit is not considered.

Fig. 10 shows the impact of the RF received power on the conversion efficiency for the three prototypes, with a load impedance of 100 kΩ. By analysing Fig. 10, on the one hand, we verify that Prototype 1 presents an average deviation between the simulated and experimental results (in terms of conversion efficiency) of around 75%, leading to a maximum conversion efficiency of 8% (for an RF received power of 3 dBm). On the other hand, Prototypes 2 and 3 present an average deviation of 40%, matching a maximum conversion efficiency of 22% (for an RF received power of 0 dBm).

The experimental results are within the simulated results, but we expected that Prototype 3 would show higher conversion efficiency results, since it considers an impedance matching circuit, compared to Prototype 2. By comparing the results between Prototype 1 and Prototype 3, the latter one shows an increase of around 15% in the conversion efficiency when considering the highest peak value for each curve. This increase in the conversion efficiency from Prototype 3 is

explained by use of a specific substrate for RF applications and by the adaptation of the length of the transmission microstrip lines that allowed optimizing the match impedance. The deviations between the simulation and experimental results are explained by the PCB manual manufacturing techniques employed to develop each prototype. Also, in simulations we consider the values supplied by the manufacturer and not the real parameter values which could induce some error in the simulation results.

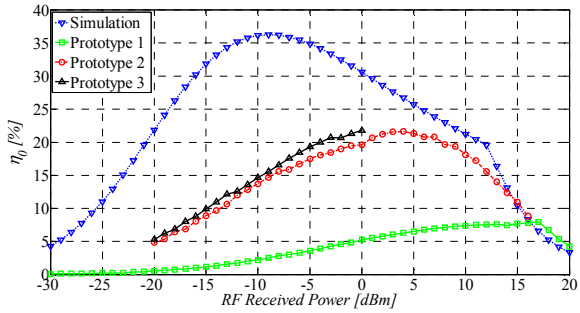

Figure 10. Impact of the RF received power on the conversion efficiency (η_0) for a 5-stage Dickson voltage multiplier with a load impedance of 100 kΩ.

By considering that the advised voltage to supply a sensor node is 3 V, Prototype 1 can power supply the sensor node for a P_r=2 dBm, with a conversion efficiency η_0≈6%. For Prototype 2 the sensor node can be power supplied for a P_r=-3 dBm, with η_0≈18%. Finally, Prototype 3 is able to supply an output voltage of 3 V for a P_r=-4 dBm, with η_0≈20%.

Combining the results and the spectral opportunities [6], the levels of received power harvested from the environment are not enough to power supply a WBAN. The data collected for the maximum levels of received power are around -27 dBm, which are insufficient to generate an output voltage of 1.8 V.

VI. CONCLUSIONS

In this paper we have identified the spectrum opportunities for RF energy harvesting in real indoor/outdoor scenarios. The set of indoor/outdoor most promising frequency bands are 79 to 96 MHz, 391 MHz, 750 to 758 MHz, 935 to 960 MHz, 1855 to 1868 MHz and 2115 to 2160 MHz. For the GSM (900/1800) frequency bands, a dual-band printed antenna has been proposed, with gains of the order of 1.8-2.06 dBi and 77.6-82% efficiency. The design of RF energy harvesting circuits and the choice of textile materials for a wearable antenna have also been analysed. Three prototypes (1, 2 and 3) for the 5-stage Dickson voltage multiplier were proposed and experimentally characterized as well as simulations of the circuits. If we consider the minimum voltage to power supply the sensor node (i.e., 1.8 V), all prototypes can power supply the necessary voltage to an IRIS *mote* work for an RF received power of -1 dBm, -7 dBm and -8 dBm, for conversion efficiencies of 5%, 16% and 17%, respectively. If the advised voltage to power supply the sensor node is considered (i.e., 3 V), all prototypes are able to power supply the sensor node for an RF received power of 2, -3 and -4 dBm, with conversion efficiencies of 6, 18 and 20%, respectively. Future work includes improving the manufacturing of the PCBs to achieve improved impedance matching whilst reaching values for the conversion efficiency closer to the simulated ones.

ACKNOWLEDGMENT

We would like to thank Prof. Luis M. Correia and Eng. Daniel Sebastião for making the NARDA-SMR spectrum analyser available to us. The contributions from Mr. Rui Barata in the production of the PCBs are also much appreciated. We also would like to thank to Eng. Ricardo Freitas from Rhode & Schwarz, for making the signal generator available to us.

REFERENCES

[1] H. Jabbar, Y. S. Song and T. T. Jeong, "RF energy harvesting system and circuits for charging of mobile devices," *IEEE Transactions on Consumer Electronics*, vol. 56, no. 1, pp. 247-253, Feb. 2010.

[2] N. Barroca, J. M. Ferro, L. M. Borges, J. Tavares and F. J. Velez, "Electromagnetic Energy Harvesting for Wireless Body Area Networks with Cognitive Radio Capabilities," in *Proc. of URSI Seminar of the Portuguese Committee*, Lisbon, Portugal, Nov. 2012.

[3] J. S. Bellon, M. Cabedo-Fabres, E. Antonino-Daviu, M. Ferrando-Bataller and F. Penaranda-Foix, "Textile MIMO antenna for Wireless Body Area Networks," in *Proc. of the 5th European Conference on Antennas and Propagation*, Rome, Italy, Apr. 2011, pp. 428-432.

[4] PROENERGY-WSN, "Prototypes for Efficient Energy Self-sustainable Wireless Sensor Networks," http://www.e-projects.ubi.pt/proenergy-wsn, Apr. 2013.

[5] J. Tavares, N. Barroca, H. M. Saraiva, L. M. Borges, F. J. Velez, C. Loss, R. Salvado, P. Pinho, R. Gonçalves and N. B. Carvalho, "Spectrum Opportunities for Electromagnetic Energy Harvesting from 350 MHz to 3 GHz," in *Proc. of The 7th International Symp. on Medical Information and Communication Technology-Special Session on Antennas and Propagation for Body Area Network*, Tokyo, Japan, Mar. 2013.

[6] N. Barroca, H. M. Saraiva, P. T. Gouveia, J. Tavares, L. M. Borges, F. J. Velez, C. Loss, R. Salvado, P. Pinho, R. Gonçalves and N. B. Carvalho, "Antennas and Circuits for Ambient RF Energy Harvesting in Wireless Body Area Networks," in *Proc. of the 24th Annual IEEE International Symposium on Personal, Indoor and Mobile Radio Communications (PIMRC'13),* London, United Kingdom, Sept. 2013.

[7] B. Annalisa and D.D.R. Danilo, *Wearable Monitoring Systems*, 1st ed., Springer, New York, USA, 2011.

[8] I. Locher, M. Klemm, T. Kirstein, and G. Troster, "Design and Characterization of Purely Textile Patch Antennas," *IEEE Transactions on Advanced Packaging*, vol. 29, no. 4, pp. 777-788, Nov. 2006.

[9] H. Yan, J. G. M. Montero, A. Akhnoukh, L. C. N. de Vreede, and J. N. Burghart, "An integration scheme for RF power harvesting," *in Proc. of The 8th Annual Workshop on Semiconductor Advances for Future Electronics and Sensors*, Veldhoven, Netherlands, Nov. 2005.

[10] Advanced Design System software, http://www.home.agilent.com/en/pc-1297113/advanced-design-system-ads?&cc=PT&lc=eng, Jan. 2013.

[11] U. Karthaus and M. Fischer, "Fully integrated passive UHF RFID transponder IC with 16.7μW minimum RF input power," *IEEE J. Solid State Circuits*, vol. 38, no. 10, pp. 1602-1608, Oct. 2003.

[12] Y. Zhou, B. Froppier and T. Razban, "Schottky Diode Rectifier for Power Harvesting Application," in *Proc. of The IEEE International Conference on RFID-Technologies and Applications*, Nice, France, Oct. 2012.

[13] P. Nintanavongsa, U. Muncuk, D. R. Lewis and K. R. Chowdhury, "Design Optimization and Implementation for RF Energy Harvesting Circuits," *IEEE Journal on Emerging and Selected Topics in Circuits and Systems*, vol. 2, no. 1, pp. 24-33, Mar. 2012.